negative differential mobility element in a circuit containing reactive elements," *J. Appl. Phys.*, vol. 43, pp. 159–172, Jan. 1972.
[4] D. D. Khandelwal and W. R. Curtice, "A study of the single-frequency quenched-domain mode Gunn-effect oscillator," *IEEE Trans. Microwave Theory Tech.*, vol. MTT-18, pp. 179–187, Apr. 1970.
[5] W. R. Curtice, "Quenched-domain mode oscillation in waveguide circuits," *IEEE Trans. Microwave Theory Tech.*, vol. MTT-21, pp. 369–374, June 1973.
[6] G. S. Hobson, "Some properties of Gunn-effect oscillations in a biconical cavity," *IEEE Trans. Electron Devices (Special Issue on Semiconductor Bulk-Effect and Transit-Time Devices)*, vol. ED-14, pp. 526–531, Sept. 1967.
[7] B. S. Perlman, "CW microwave amplification from circuit-stabilized epitaxial GaAs transferred-electron devices," *IEEE J. Solid-State Circuits (Special ISSCC Issue on Solid-State Microwave Circuits)*, vol. SC-5, pp. 331–337, Dec. 1970.
[8] K. R. Freeman and G. S. Hobson, "A survey of CW and pulsed Gunn oscillators by computer simulation," *IEEE Trans. Electron Devices*, vol. ED-20, pp. 891–903, Oct. 1973.
[9] P. Jeppesen and B. Jeppsson, "The influence of diffusion on the stability of supercritical transferred electron amplifiers," *Proc. IEEE* (Lett.), vol. 60, pp. 452–454, Apr. 1972.
[10] R. A. Kiehl, "The internal dynamics and microwave properties of *X*-band transferred-electron devices," Ph.D. dissertation, Purdue Univ., Lafayette, IN, 1974.
[11] J. G. Ruch and W. Fawcett, "Temperature dependence of the transport properties of gallium arsenide determined by a Monte Carlo method," *J. Appl. Phys.*, vol. 41, pp. 3845–3850, Aug. 1970.
[12] P. Jeppesen and B. I. Jeppsson, "A simple analysis of the stable field profile in the supercritical TEA," *IEEE Trans. Electron Devices*, vol. ED-20, pp. 371–379, Apr. 1973.
[13] J. A. Copeland and S. Knight, "Applications utilizing bulk negative resistance," in *Semiconductors and Semimetals*, vol. 7A, R. K. Williardson and A. C. Beer, Ed. New York: Academic, 1971, pp. 3–72.
[14] H. Kroemer, "Nonlinear space-charge domain dynamics in a semiconductor with negative differential mobility," *IEEE Trans. Electron Devices (Special Issue on Semiconductor Bulk-Effect and Transit-Time Devices)*, vol. ED-13, pp. 27–40, Jan. 1966.
[15] K. Blotekjaer, "Transport equations for electrons in two-valley semiconductors," *IEEE Trans. Electron Devices*, vol. ED-17, pp. 38–47, Jan. 1970.
[16] D. Jones and H. D. Rees, "Electron-relaxation effects in transferred-electron devices revealed by new simulation method," *Electron. Lett.*, vol. 8, pp. 363–364, July 1972.
[17] K. Kurokawa, "Some basic characteristics of broadband negative resistance oscillator circuits," *Bell Syst. Tech. J.*, vol. 48, pp. 1937–1955, July 1969.
[18] C. P. Jethwa and R. L. Gunshor, "An analytical equivalent circuit representation for waveguide-mounted Gunn oscillators," *IEEE Trans. Microwave Theory Tech.*, vol. MTT-20, pp. 565–572, Sept. 1972.
[19] R. L. Eisenhart and P. J. Khan, "Some tuning characteristics and oscillation conditions of waveguide-mounted transferred-electron diode oscillator," *IEEE Trans. Electron Devices*, vol. ED-19, pp. 1050–1055, Sept. 1972.
[20] R. P. Owens and D. Cawsey, "Microwave equivalent-circuit parameters of Gunn-effect-device packages," *IEEE Trans. Microwave Theory Tech., (Special Issue on Microwave Circuit Aspects of Avalanche-Diode and Transferred Electron Devices)*, vol. MTT-18, pp. 790–798, Nov. 1970.

Filters with Single Transmission Zeros at Real or Imaginary Frequencies

RALPH LEVY, FELLOW, IEEE

Abstract—**A new unified theory is presented for the synthesis of exactly equiripple low-pass prototypes having: a) one simple pole of attenuation at a real frequency; or b) a single pair of real-axis transmission zeros (giving linear-phase performance). These types of filters may be regarded as representing the least possible degree of complication over the conventional Chebyshev filter, and are usually realized with one extra cross coupling in the structure. It is demonstrated that this gives much improved skirt selectivity in the case of a finite frequency pole, making it a viable intermediate case between the Chebyshev and elliptic-function filters, while in the case of real-frequency zeros, very flat group delay over 50 percent of the passband is achieved with minimal cost in insertion loss and skirt rejection. Approximate and exact synthesis techniques are described, including results for the previously neglected odd-degree case. Experimental results demonstrate agreement with theory.**

I. Introduction

THIS PAPER describes two classes of filters which have quite distinct applications, yet are closely related mathematically and in physical realization. They are distinguished by the location of their transmission zeros (attenuation poles), which, in the case of the first class, are at real frequencies, and in the case of the second class are at imaginary frequencies (i.e., on the real axis of the complex frequency plane). In this paper filters having only one pair of transmission zeros are described, not only because these cases may be synthesized exactly with no difficulty, but also because they give important substantial improvements compared with conventional Chebyshev equiripple filters, yet with little practical difficulty of physical realization.

The transmission zeros may be realized by cross coupling a pair of nonadjacent elements of the filter, negatively to give real-frequency transmission zeros, positively to give real-axis zeros. The first type of filter gives improved skirt attenuation performance, and the second gives improved passband delay characteristics compared with the ordinary Chebyshev filter.

The first application of coupling between nonadjacent resonators at microwave frequencies appears to have originated with Kurzrok [1], [2]. He showed that to obtain finite frequency attenuation poles it was necessary to

Manuscript received July 18, 1975; revised October 27, 1975.
The author is with the Microwave Development Laboratories, Natick, MA 01760.

reverse the "natural" phase of the extra cross coupling. It was not until much later that Rhodes [3] showed that when the cross couplings have the same phase as the direct couplings then the finite transmission zeros produced are either complex or on the real axis of the complex frequency plane. Hence they may be used to design filters having nonminimum-phase characteristics, e.g., linear-phase filters [4]. Other authors have employed cross couplings to realize elliptic-function filters, and recently more general types having both finite attenuation poles and delay equalization have been described [5]–[7].

Filters with several cross couplings tend to be relatively difficult to tune, encouraging some designers to look at the possibility of synthesizing high-ordered filters having just one or two finite frequency transmission zeros [8], [9]. However, the low-pass filters discussed in [8] are not equiripple and are therefore nonoptimum. The bandpass filters described by Cristal [9] are for a somewhat limited application (interdigital filters of broad bandwidth) and require extra resonant elements rather than cross couplings.

II. Approximation Functions for Single-Pole Filters

A. Filters with a Real-Frequency Attenuation Pole

It is perhaps surprising that the low-pass rational function to be introduced apparently has not been utilized previously, at least for the applications described here, since it is derived by a straightforward application of Chebyshev's theorem, a brief description of which may be found in [10]. The rational function has simple poles at $x = \pm a$, and takes the form

$$f(x) = \frac{P_n(x)}{a^2 - x^2} \tag{1}$$

where $P_n(x)$ is a polynomial of degree n. It is shown schematically in Fig. 1 for the case $n = 8$ with a real value for the parameter a. Application of Chebyshev's theorem gives the function (1) specifically in the form

$$f(x) = \cos [(n - 2)\phi + 2\theta] \tag{2}$$

where

$$\cos \phi = x \tag{3}$$

$$\cos \theta = \frac{x\sqrt{a^2 - 1}}{\sqrt{a^2 - x^2}} \tag{4}$$

$$\sin \theta = \frac{a\sqrt{1 - x^2}}{\sqrt{a^2 - x^2}} \tag{5}$$

which may be expressed in terms of Chebyshev functions as

$$f(x) = \frac{(a + \sqrt{a^2 - 1})^2 x T_{n-1}(x) + (a - \sqrt{a^2 - 1})^2 x T_{n-3}(x) - 2a^2 T_{n-2}(x)}{2(a^2 - x^2)}. \tag{6}$$

This rational form is used in the exact synthesis method of Section III-B. The low-pass prototype filter has an insertion loss given by

$$A = 1 + h^2 f^2(x) \tag{7}$$

where h is small for small passband ripple levels, and the maximum passband return loss is defined as

$$A_R = 10 \log_{10} (1 + 1/h^2) \quad \text{dB}. \tag{8}$$

The location of the stopband minimum shown in Fig. 1 is derived by differentiation of (2) or (6), giving

$$x_2^2 = a^2 + 2a\sqrt{a^2 - 1}/(n - 2) \tag{9}$$

and the filter attenuation at this minimum is, therefore,

$$A_S = 10 \log_{10} [1 + h^2 f^2(x_2)] \quad \text{dB}. \tag{10}$$

Since $1/h^2 \gg 1$ and $h^2 f^2(x_2) \gg 1$, we have

$$A_R + A_S \simeq 20 \log_{10} f(x_2) \quad \text{dB} \tag{11}$$

which is independent of the passband ripple level.

The edge of the stopband is the value x_1 indicated in Fig. 1, and is derived numerically by iteration. This enables the value of $A_R + A_S$ given by (11) to be plotted as a function of x_1, as shown in Fig. 2 for filters of degree 3 through 10. Similar graphs are available for Chebyshev and optimum elliptic-function filters [11], and when the characteristics of the three types of filters are compared it is found that for any given degree they are almost exactly parallel to one another. This is illustrated in Fig. 3, which compares elliptic-function, single-pole, and Chebyshev filters all of degree 8. Here it is seen that the Chebyshev-filter plot of

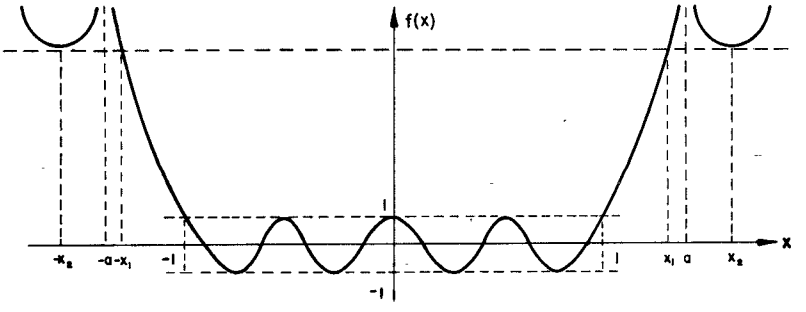

Fig. 1. Rational function with single pole (case $n = 8$).

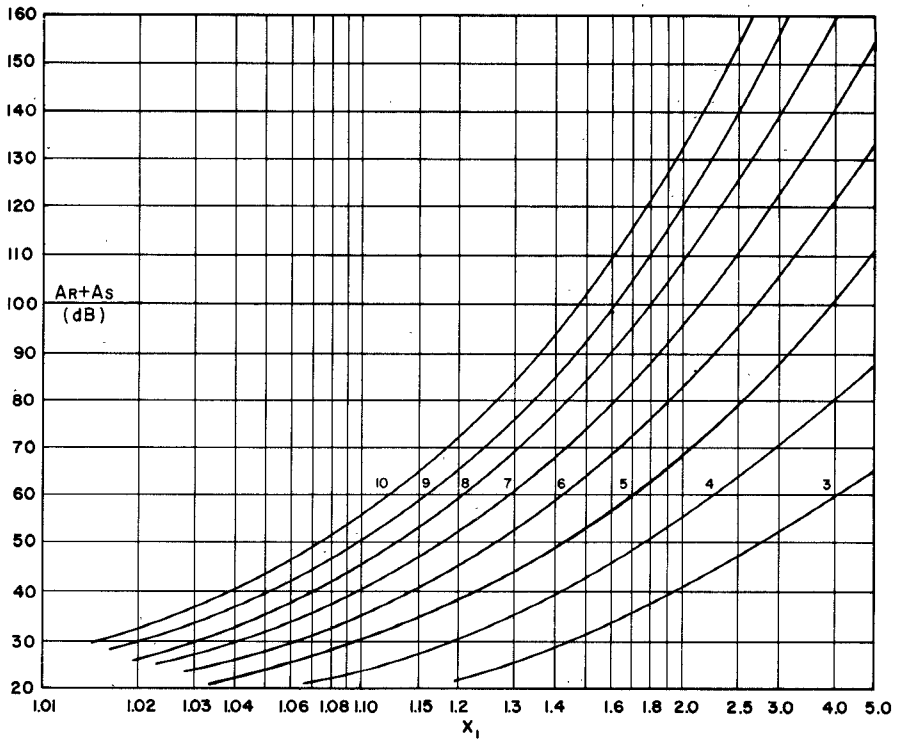

Fig. 2. Universal characteristics for single-pole filters.

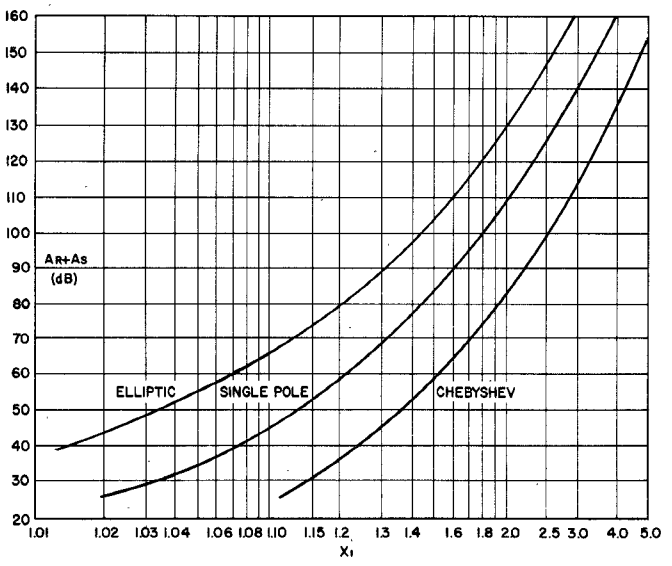

Fig. 3. Comparison of 8th-degree-elliptic, single-pole, and Chebyshev filters.

$A_R + A_S$ parallels that of the single-pole filter at ordinate values approximately 22 dB lower, and the elliptic filter parallels the single-pole filter at ordinate values approximately 18 dB higher. The ordinate differences between the three types of filters are given in Table I. Note that the single-pole filters of degrees 3 and 4 are identical to the elliptic filter, as expected. The improvement in skirt attenuation over a Chebyshev filter upon introducing finite poles is quite large when one finite pole is introduced, and becomes successively less as subsequent poles are introduced. Evidently the extra complexity of the elliptic-function filter compared with the single-pole filter may not always be justified.

TABLE I
ATTENUATION DIFFERENCES BETWEEN SINGLE-POLE FILTERS AND CHEBYSHEV AND ELLIPTIC FILTERS AT THE STOPBAND EDGE FREQUENCY

n	3	4	5	6	7	8	9	10
Chebyshev (dB)	-12	-15	-17.5	-19	-21	-22	-23	-24
Elliptic (dB)	0	0	6	9	15	18	24	27
No. of finite freq poles in elliptic filter	1	1	2	2	3	3	4	4

The physical realization and synthesis of the element values of this low-pass prototype are described in Section III.

B. Filters with Real-Axis Transmission Zeros (Linear-Phase Filters)

Here the mathematical similarity between the two classes of filters becomes apparent, since it is necessary only to take the function (6) and make the substitution

$$a = j\sigma \tag{12}$$

where σ is real. The function becomes

$$f(x) = \frac{(\sqrt{\sigma^2 + 1} + \sigma)^2 x T_{n-1}(x) + (\sqrt{\sigma^2 + 1} - \sigma)^2 x T_{n-3}(x) - 2\sigma^2 T_{n-2}(x)}{2(\sigma^2 + x^2)}. \tag{13}$$

Hence the insertion loss function for an equiripple low-pass filter having a pair of real-axis transmission zeros at $x = \pm j\sigma$ is

$$A = 1 + h^2 f^2(x). \tag{7}$$

The introduction of the real-axis transmission zeros has a large effect on the phase characteristics of this filter compared to a similar Chebyshev filter. If the value of σ is chosen correctly, then the group-delay characteristic in the low-pass band becomes very flat over approximately 50 percent of the band, and also is improved over the rest of the band. It is possible to realize group-delay curves corresponding to undercoupled, critically coupled, and overcoupled characteristics. Not surprisingly the optimum value for σ is quite close to unity. The group delay may be calculated from the synthesized circuit, and by slight adjustment of σ it is possible to iterate rapidly to the desired delay characteristic.

In this case the skirt attenuation is less than that of the Chebyshev filter of identical degree. In practice it is found that for values of σ near unity, giving a flat delay characteristic, and for attenuation values in the useful range of about 20–80 dB, the skirt attenuation of the nth-degree linear-phase filter is almost identical to that of the standard Chebyshev filter of degree $(n - 1)$. Hence it is hardly necessary to present special curves for this type of linear-phase filter. An example design is presented in Section V.

III. Synthesis of Single-Pole Prototype Filters

The basic low-pass prototype filters may be synthesized as the circuits shown in Fig. 4(b) for n odd, and in Fig. 4(a) for n even. These are the admittance-inverter equivalent circuits [4], where the rectangular boxes represent ideal admittance inverters. The central elements of the circuit for n odd are given primed values (g_m', g_{m+1}', C_m') since alternative equivalent circuits will be presented in this case

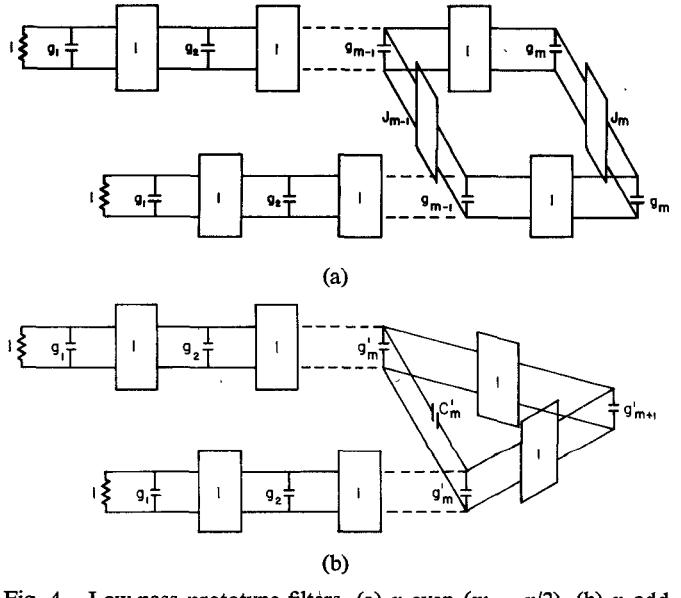

Fig. 4. Low-pass prototype filters. (a) n even ($m = n/2$). (b) n odd ($m = (n - 1)/2$).

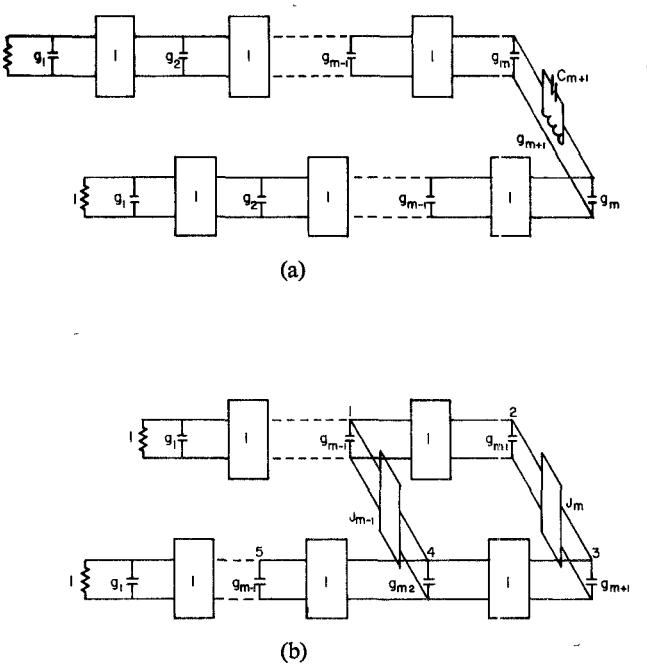

Fig. 5. Equivalent circuits for n odd. (a) n odd (alternative symmetrical realization). (b) n odd (asymmetrical realization).

(see Fig. 5). The extra cross-coupling inverter of admittance J_{m-1} is positive for the linear-phase filter, and negative for the filter having a real-frequency pole. The extra cross-coupling capacitance C_m' is also positive for the linear-phase filter and negative for the single-pole filter. Hence it cannot give a direct practical realization of the single-pole filter. In this case, one of the equivalent circuits presented in Fig. 5 could be used.

In the previous statements the term "extra" denotes the fact that the extra cross coupling is not present in the case of a conventional Chebyshev filter, and that this cross-coupling element represents the only extra feature in the new design.

Before describing results for the exact synthesis, an approximate synthesis technique will be presented, which is particularly useful for the case of linear-phase filters.

A. Approximate Synthesis

This may be achieved by introducing cross coupling between one pair of nonadjacent elements of the standard Chebyshev filter while leaving all but one of the elements unchanged. In the case of n even, where the low-pass prototype filter is shown in Fig. 4(a), the element values are given by the well-known formulas

$$g_1 = \frac{2 \sin \frac{\pi}{2n}}{\gamma}$$

$$g_r g_{r-1} = \frac{4 \sin \frac{(2r-1)\pi}{2n} \sin \frac{(2r+1)\pi}{2n}}{\gamma^2 + \sin^2 \frac{r\pi}{n}},$$

$$(r = 1,2,\cdots,m), \qquad m = n/2$$

$$\gamma = \sinh\left(\frac{1}{n}\sinh^{-1}\frac{1}{h}\right)$$

$$S = (\sqrt{1+h^2}+h)^2 \quad \text{(the passband VSWR)}$$

$$J_m = \sqrt{S}\cdots m \quad \text{odd or} \quad 1/\sqrt{S}\cdots m \quad \text{even}$$

$$J_{m-1} = 0\cdots \quad \text{for Chebyshev filters.} \tag{14}$$

In order to introduce transmission zeros at $\omega = \pm a$, the required value of J_{m-1} is given by

$$J_{m-1} = \frac{-J_m'}{(ag_m)^2 - J_m'^2} \tag{15}$$

where J_m' is a slightly changed value of J_m as in (17). This formula holds for both negative and positive cross coupling, i.e., for $a = j\sigma$

$$J_{m-1} = \frac{J_m'}{(\sigma g_m)^2 + J_m'^2}. \tag{16}$$

Introduction of J_{m-1} mismatches the filter, and to maintain a good VSWR at midband it is necessary to change the value of J_m slightly according to the formula

$$J_m' = \frac{J_m}{1 + J_m J_{m-1}}. \tag{17}$$

No other elements of the original Chebyshev filter are changed. The proof of the equations (15)–(17) is given in Appendix I.

Typical results for this approximate design procedure are shown in Figs. 6 and 7. In each case the original Chebyshev

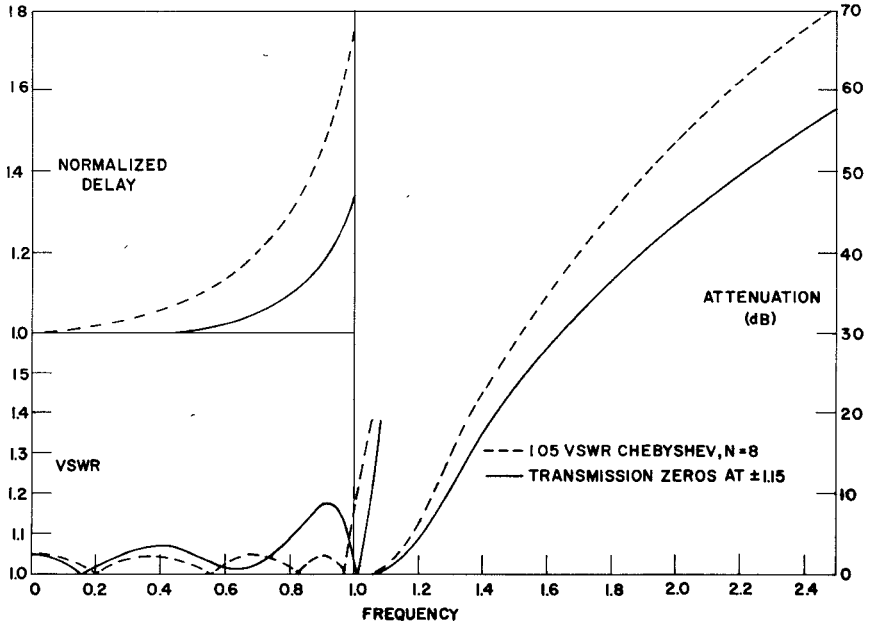

Fig. 6. Introduction of real-axis transmission zeros.

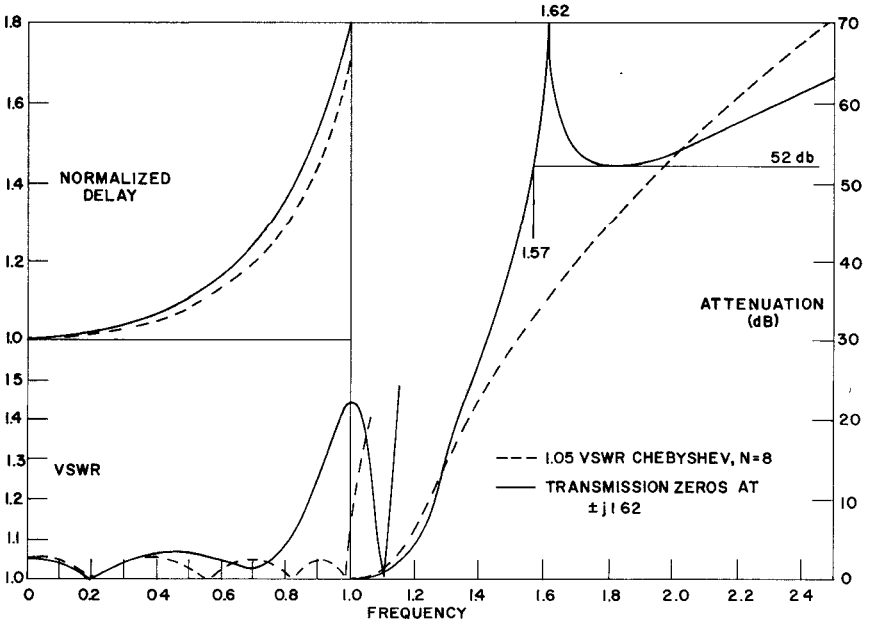

Fig. 7. Introduction of real-frequency transmission zeros.

prototype filter is of degree $n = 8$, and a ripple VSWR of 1.05 is chosen, in accordance with typical specifications for modern communications filters. In the case of the linear-phase design depicted in Fig. 6 having transmission zeros at $\sigma = \pm 1.07$, the delay is essentially flat over 50 percent of the passband, and the VSWR has deteriorated only slightly. The exact element values derived by synthesis are compared with the approximate values in Table II, and differ at most by 3 percent. The implication here is that the approximate theory may be used with confidence for linear-phase prototypes, especially knowing that the element values of a bandpass filter based upon the design will tune to give the desired exact equiripple VSWR characteristic, since in practice the various couplings need to be slightly readjusted as part of the tuning process.

The result of introducing a finite attenuation pole at $\omega = 1.62$, as shown in Fig. 7, is not quite as satisfactory with the approximate theory. The VSWR has deteriorated to a greater extent, and the cutoff frequency has increased by approximately 10 percent. It is possible to amend (17) to force a perfect match at band edge, but it is found that the in-band VSWR is still quite poor compared with the specification. The approximate and exact element values given in Table II show quite large differences for the central elements (5 percent for g_4 and J_4, 22 percent for J_3), and bandpass filters based on the approximate design would tend to have the large VSWR ripples near the band edges in practice.

Another, perhaps more compelling, requirement for an exact synthesis is that in the latter case (real-frequency poles), (15) and (17) do not have a reasonable solution when an attempt is made to move the finite pole closer to the edge of the passband. Thus in the case of our $N = 8$, VSWR = 1.05 example, it is impossible to move the pole closer than $\omega = 1.53$. Of course since the filter cutoff increases beyond unity the renormalized pole value is actually less than 1.53, but the VSWR deteriorates quite severely. The fact that the VSWR is not exactly equiripple causes substantial reduction in skirt attenuation, i.e., optimality is lost.

B. Exact Synthesis

This may be carried out using the standard Darlington procedure, i.e., the input reflection coefficient Γ is derived from (6), (7) or (7), (13) as

$$\Gamma^2 = \frac{h^2 f^2(x)}{1 + h^2 f^2(x)}. \tag{18}$$

The substitution $x = -jp$ is made, and a Hurwitz factorization of the denominator carried out. This process may be simplified and the accuracy increased if due note is taken of the fact that the denominator polynomial is of even degree ($= 2n$), and the factorization can take place in the p^2 variable. Then the square root of each p_i^2 root factor is formed, and the ones with nonpositive real parts taken to form the Hurwitz polynomial. No factorization of the numerator polynomial is required. The driving point impedance is given by

$$Z(p) = \frac{1 + \Gamma(p)}{1 - \Gamma(p)} \tag{19}$$

from which the transfer matrix may be formed. Synthesis of the prototypes shown in Fig. 4 is carried out by extracting elements from each side of the filter until the central region is reached. In the case of n even, extraction is carried out including elements g_{m-1} of Fig. 4(a), and for n odd including the elements g_m' of Fig. 4(b). The central elements may then be written down by inspection of the remainder transfer matrix.

Results for the exact synthesis corresponding to cases considered previously for the approximate synthesis are presented in Table II. Here it is seen that the major deviations occur in the central part of the filter (elements g_4, J_3, and J_4).

C. Pole Locations

The changes which occur in the location of the complex-frequency-plane poles of the transfer function upon introducing the real-frequency and real-axis transmission zeros are shown in Fig. 8. Here the upper-left half-plane is shown, and the poles are plotted for the Chebyshev prototype and for the two other cases previously discussed in this paper (i.e., the exact cases of Table II). The most interesting feature is that in the linear-phase (real-axis zeros) case the poles tend to migrate to the vertical dotted line shown. In the more complex type of linear-phase filters having several extra cross couplings, the poles tend to lie on this vertical line with almost equal vertical spacing [7].

IV. Equivalent Circuits for n Odd

Most of the linear-phase filters described in the previous literature have been restricted to the even-degree case, since it is often difficult to realize the circuit shown in Fig. 4(b) in a direct manner. However, this circuit has the exact

TABLE II
Comparison of Approximate and Exact Designs: $n = 8$, VSWR = 1.05

	$p=\infty$	$p=\pm 1.07$		$p=\pm j1.62$	
	Chebyshev	Approx.	Exact	Approx.	Exact
g_1	0.67377	0.67377	0.66743	0.67377	0.67936
g_2	1.33553	1.33553	1.32113	1.33553	1.34808
g_3	1.65623	1.65623	1.63253	1.65623	1.67622
g_4	1.65657	1.65657	1.69047	1.65657	1.74317
J_3	0	0.21300	0.20659	-0.22048	-0.18015
J_4	0.97590	0.80795	0.81216	1.24344	1.18407

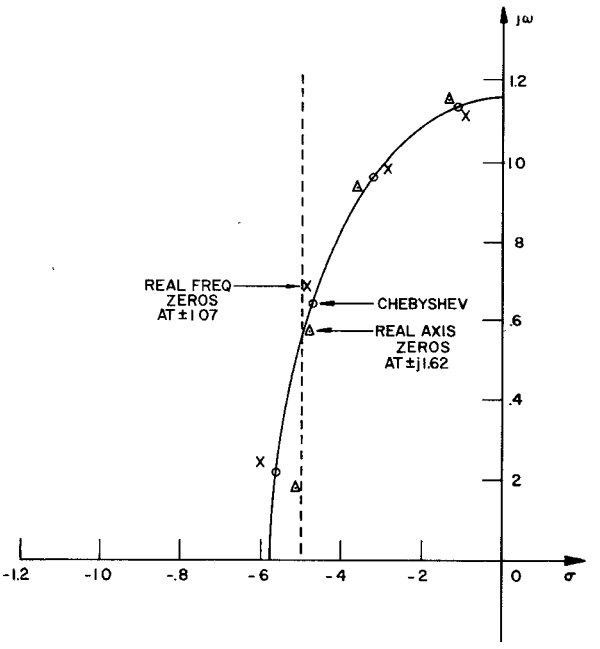

Fig. 8. Pole locations, $n = 8$, VSWR = 1.05.

equivalent shown in Fig. 5(b), which is similar to the even-degree realization of Fig. 4(a). The main difference is the existence of one more element on the lower side of the central rectangle compared with the upper side. Note that if the circuit of Fig. 4(a) is converted into a bandpass filter by means of a low-pass to bandpass transformation, then the cross-coupling susceptance $\omega C_m'$ transforms into a resonant element rather than the desired frequency-independent cross coupling. This difficulty does not arise with the circuit of Fig. 5(b), which is a prototype yielding band-pass linear-phase filters which are no more complicated than those of even degree. The existence of this simple odd-degree prototype results in extra design flexibility.

The circuit shown in Fig. 5(a) is also of interest, being a direct lumped-element filter having no cross coupling, i.e., it possesses the more conventional low-pass prototype format. The element values of these equivalent circuits may be expressed in terms of those given in Fig. 4(b). It is simple to convert circuit 4(b) into 5(a), since combining the two admittance inverters with g'_{m+1} in 4(b) gives the transfer matrix

$$\begin{pmatrix} 0 & j \\ j & 0 \end{pmatrix} \begin{pmatrix} 1 & 0 \\ jg'_{m+1}\omega & 1 \end{pmatrix} \begin{pmatrix} 0 & j \\ j & 0 \end{pmatrix} = \begin{pmatrix} -1 & -jg'_{m+1}\omega \\ 0 & -1 \end{pmatrix}. \quad (20)$$

This represents a series inductance g'_{m+1} in cascade with a $1:-1$ ideal transformer. The capacitor C_m' is added in parallel with this circuit, and elimination of the $1:-1$ transformer has the effect of changing the sign of C_m'. (This statement may be proved by synthesizing the circuit in the two ways.) Thus the result is

$$g_m = g_m' \qquad g'_{m+1} = g'_{m+1} \qquad C_{m+1} = -C_m'. \quad (21)$$

Hence to obtain real-frequency transmission zeros, C_{m+1} is positive in Fig. 5(a), but C_m' is negative in Fig. 4(b), and not realizable in the latter case. The opposite situation holds for real transmission zeros.

Returning to the circuit of Fig. 5(b), which, as stated, is of greater practical interest, the element values are expressible in terms of those given in Fig. 4(b) as follows:

$$J_{m-1} = \frac{C_m'}{g_m' + C_m'} = \frac{C_m'}{g_{m1}} \quad (22)$$

$$J_m = 1/(1 + J_{m-1}) \quad (23)$$

$$g_{m1} = g_m' + C_m' \quad (24)$$

$$g_{m2} = g_m'(1 + J_{m-1}) = g_m'/J_m \quad (25)$$

$$g_{m+1} = \frac{g'_{m+1}}{(1 + J_{m-1})^2} = J_m^2 g'_{m+1}. \quad (26)$$

The proof of these equations is given in Appendix II.

There is also the relationship for the location of the transmission zeros, which from Fig. 4(b) is given as

$$a^2 = \frac{-1}{g'_{m+1}C_m'}. \quad (27)$$

Substituting for g'_{m+1} and C_m' from (26) and (22) gives

$$J_{m-1} = \frac{-J_m^2}{a^2 g_{m1} g_{m+1}}. \quad (28)$$

This can be reexpressed in more revealing terms using (23) as

$$J_{m-1} = \frac{-J_m}{a^2 g_{m1} g_{m+1} - J_m^2} \quad (29)$$

which is similar to the expression (15) derived for the even-degree case.

V. Experimental Results

The first realization of microwave bandpass filters having finite real-frequency attenuation poles were described by Kurzrok [1], [2]. Other realizations using waveguide cavities [5] or combline [6] are also feasible. The combline structure is a particularly neat and simple solution for

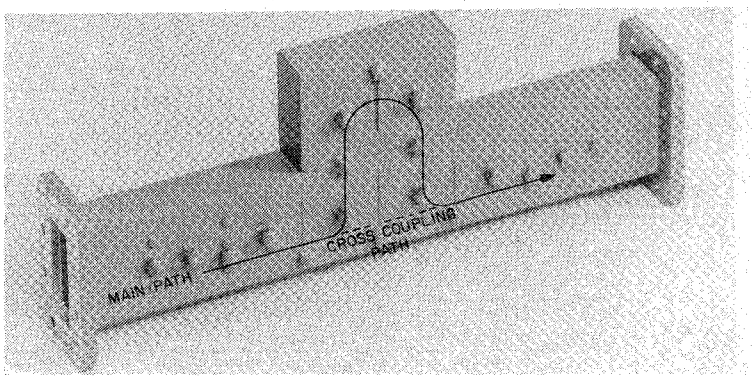

Fig. 9. 8-cavity WR137 waveguide linear-phase filter.

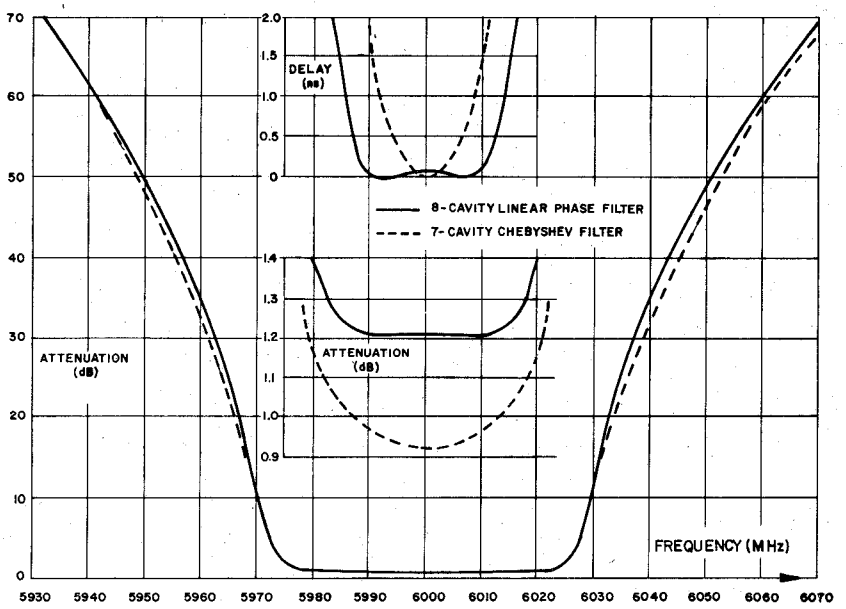

Fig. 10. Comparison of 8-cavity linear-phase filter with 7-cavity Chebyshev filter.

coaxial or TEM line filters when finite frequency poles are required. These require the addition of one cross-coupling capacitor.

Most of the practical results obtained by the author are for filters having real-axis transmisson zeros. The design of bandpass filters for the more general case has been described by Rhodes [4], and these design techniques also apply to the case where only one extra cross coupling is present. Hence there is no need to repeat this theory here. As stated previously, the main advantage of having just one extra cross coupling lies in the ease of tuning, with some advantage to be gained, particularly in the case of waveguide filters, in having a more convenient physical layout.

The mechanical construction of an 8-cavity waveguide filter in WR137 is shown in Fig. 9, and its performance, compared with that of a 7-cavity Chebyshev filter having the same bandwidth and ripple level, is shown in Fig. 10. The improved amplitude and delay of the self-equalized filter are obtained at the cost of slightly increased insertion loss and the loss of "one cavity" of attenuation compared with the Chebyshev filter, as stated in Section II-B. This filter is designed using the $n = 8$, ripple VSWR = 1.05 prototype with transmission zeros located at ± 1.07 (see Table II). The equiripple bandwidth is 46 MHz, and the flat-delay bandwidth is seen to be 50 percent of this, in agreement with the theory. This delay characteristic, shown in Fig. 10, is seen to possess an overcoupled characteristic, but it is quite simple to tune it to have more or less such overcoupling [12].

Similar filters have been constructed using high-Q TE_{011}-mode cylindrical cavities, and in interdigital form.

VI. Conclusions

The results presented demonstrate an interesting unification of the theories for the two cases of real-frequency or real-axis (imaginary frequency) transmission zeros. The approximate synthesis given is very simple to apply, and is sufficiently precise for many practical applications.

In the case of the real-frequency attenuation pole, the universal design curves given in Fig. 2 may be compared with those previously published for elliptic-function and Chebyshev filters. The results are shown to have an intermediate character, as demonstrated in Fig. 3. The single-pole filter should be considered a viable alternative to the more complicated elliptic-function design.

The case of real-axis transmission zeros gives the simplest

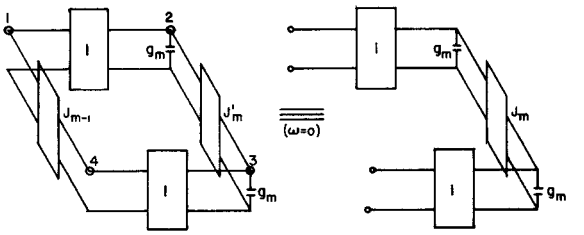

Fig. 11. Matching condition to be established (approximate theory).

possible linear-phase filter, simple in both physical realization and in ease of tuning, yet gives a vast improvement in passband group delay compared with a Chebyshev filter of equal skirt rejection performance.

The results presented for the odd-degree case, and especially the equivalent circuit of Fig. 5(b), give improved design flexibility since it is no longer necessary to jump two degrees to obtain greater skirt rejection.

These results have been extended to singly terminated and other types of physically asymmetric filters used in diplexers. This extension is rather obvious, and results are not presented in this paper. Such linear-phase diplexers have been constructed and give results in agreement with predictions.

Appendix I

The central portion of the network is shown in Fig. 11(a). The admittance matrix is

$$j\begin{bmatrix} 0 & -1 & 0 & -J_{m-1} \\ -1 & g_m\omega & -J_m' & 0 \\ 0 & -J_m' & g_m\omega & -1 \\ -J_{m-1} & 0 & -1 & 0 \end{bmatrix}. \tag{30}$$

In order to obtain the two-port admittance matrix between the input and output ports, it is necessary to eliminate the 12, 13, 42, and 43 entries in (30), (the 13 and 42 entries are already zero). This can be accomplished by adding a suitable linear combination of rows 2 and 3 to rows 1 and 4. Thus if we take $k_1 \times$ row 2 and $k_2 \times$ row 3 and add to row 1 we obtain a new row 1 as

$$j(-k_1,\ -1 + k_1 g_m\omega - k_2 J_m',\ -k_1 J_m' + k_2 g_m\omega, - J_{m-1} - k_2). \tag{31}$$

The second and third entries in (31) are zero if we choose

$$k_1 = \frac{1}{g_m\omega - \dfrac{J_m'^2}{g_m\omega}} \qquad k_2 = \frac{J_m'}{(g_m\omega)^2 - J_m'^2} \tag{32}$$

and the admittance matrix of Fig. 11(a) between the input and output ports is therefore

$$-j\begin{bmatrix} k_1 & k_2 + J_{m-1} \\ k_2 + J_{m-1} & k_1 \end{bmatrix}. \tag{33}$$

The condition for no transmission is that the off-diagonal entries be zero, this occurring at a frequency $\omega = a$, giving (15) as required.

The value of J_m' is to be chosen to match the circuit at $\omega = 0$, i.e., the equivalence of Fig. 11 must be established. The admittance matrix of network 11(b) is the same as (33) with $J_{m-1} = 0$ and with the prime dropped from J_m' in (32). This leads immediately to the matching condition (17).

Appendix II

The admittance matrix of the central 5 nodes of the circuit in Fig. 4(b), neglecting elements g_{m-1}, is

$$j\begin{bmatrix} 0 & -1 & 0 & 0 & 0 \\ -1 & (g_m' + C_m')\omega & -1 & -C_m'\omega & 0 \\ 0 & -1 & g'_{m+1}\omega & -1 & 0 \\ 0 & -C_m'\omega & -1 & (g_m' + C_m')\omega & -1 \\ 0 & 0 & 0 & -1 & 0 \end{bmatrix}. \tag{34}$$

This may be converted to the circuit indicated as nodes 1–5 in Fig. 5(b) by eliminating the 24 coupling and introducing 14 coupling. The first step in this process is to add column 2 multiplied by the factor $C_m'/(g_m' + C_m')$ to column 4, plus a similar operation with respect to rows 2 and 4, giving the admittance matrix

$$j\begin{bmatrix} 0 & -1 & 0 & \dfrac{-C_m'}{g_m' + C_m'} & 0 \\ -1 & (g_m' + C_m')\omega & -1 & 0 & 0 \\ 0 & -1 & g'_{m+1}\omega & -\left(1 + \dfrac{C_m'}{g_m' + C_m'}\right) & 0 \\ \dfrac{-C_m'}{g_m' + C_m'} & 0 & -\left(1 + \dfrac{C_m'}{g_m' + C_m'}\right) & \left(g_m' + \dfrac{C_m' g_m'}{g_m' + C_m'}\right)\omega & -1 \\ 0 & 0 & 0 & -1 & 0 \end{bmatrix}. \tag{35}$$

The second step is to make the admittance inverter 34 unity by multiplying row 3 and column 3 by $1/(1 + J_{m-1})$ where $J_{m-1} = C_m'/(g_m' + C_m')$, giving the final admittance matrix representing the 5 nodes of Fig. 5(b) as

$$j\begin{bmatrix} 0 & -1 & 0 & \dfrac{-C_m'}{g_m' + C_m'} & 0 \\ -1 & (g_m' + C_m')\omega & \dfrac{-1}{1 + J_{m-1}} & 0 & 0 \\ 0 & \dfrac{-1}{1 + J_{m-1}} & \dfrac{g_{m+1}'\omega}{(1 + J_{m-1})^2} & -1 & 0 \\ \dfrac{-C_m'}{g_m' + C_m'} & 0 & -1 & \left(g_m' + \dfrac{C_m' g_m'}{g_m' + C_m'}\right)\omega & -1 \\ 0 & 0 & 0 & -1 & 0 \end{bmatrix}. \tag{36}$$

Equations (22)–(26) may now be written down by inspection of matrix (36).

Acknowledgment

The author wishes to thank Dr. E. G. Cristal for discussions, and Dr. H. J. Riblet for his support during this work.

References

[1] R. M. Kurzrok, "General three-resonator filters in waveguide," *IEEE Trans. Microwave Theory Tech.* (Corresp.), vol. MTT-14, pp. 46–47, Jan. 1966.

[2] ——, "General four-resonator filters at microwave frequencies," *IEEE Trans. Microwave Theory Tech.* (Corresp.), vol. MTT-14, pp. 295–296, June 1966.

[3] J. D. Rhodes, "The theory of generalized interdigital networks," *IEEE Trans. Circuit Theory*, vol. CT-16, pp. 280–288, Aug. 1969.

[4] a) ——, "A low-pass prototype network for microwave linear phase filters," *IEEE Trans. Microwave Theory Tech.*, vol. MTT-18, pp. 290–300, June 1970.
b) ——, "The generalized interdigital linear phase filter," *ibid.*, vol. MTT-18, pp. 300–307, June 1970.
c) ——, "The generalized direct-coupled cavity linear phase filter," *ibid.*, vol. MTT-18, pp. 308–313, June 1970.

[5] A. E. Atia and A. E. Williams, "Nonminimum-phase optimum amplitude bandpass waveguide filters," *IEEE Trans. Microwave Theory Tech.*, vol. MTT-22, pp. 425–431, Apr. 1974.

[6] R. Levy, "Mixed lumped and distributed linear phase filters," in *Proc. 1974 European Conf. Circuit Theory and Design*, Inst. Elec. Eng. (London), Conf. Pub. 116, pp. 32–37.

[7] R. J. Wenzel, "Solving the approximation problem for narrow-band bandpass filters with equal-ripple passband response and arbitrary phase response," in *1975 IEEE MTT-S Int. Microwave Symp. Dig.*, p. 50 (IEEE catalog no. 75CH0955-5MTT).

[8] M. C. Agarwal and A. S. Sedra, "On designing sharp cut-off low-pass filters," *IEEE Trans. Audio Electroacoust.*, vol. AU-20, pp. 138–141, June 1972.

[9] E. G. Cristal, "Design equations for a class of wide-band bandpass filters," *IEEE Trans. Microwave Theory Tech.* (Short Papers), vol. MTT-20, pp. 696–699, Oct. 1972.

[10] R. Levy, "Generalized rational function approximation in finite intervals using Zolotarev functions," *IEEE Trans. Microwave Theory Tech. (1970 Symp. Issue)*, vol. MTT-18, pp. 1052–1064, Dec. 1970.

[11] R. Saal, "Der Entwurf von filtern mit halfe des Kataloges normierter tiefpässe," Telefunken A.G., Backnang (Württenberg), Germany, 1966, pp. 7, 8.

[12] R. Levy, "Phase equalized filter," U.S. Patent 3 882 434, May 6, 1975.